Closed-loop correction and ocular wavefronts compensation of a 62-element silicon unimorph deformable mirror

Jianqiang Ma (马剑强)[1,2,3,*], Kai Chen (陈 凯)[1,2], Junjie Chen (陈俊杰)[3], Baoqing Li (李保 庆)[3], and Jiaru Chu (褚家如)[3]

[1]*Faculty of Mechanical Engineering and Mechanics, Ningbo University, Ningbo 315211, China*
[2]*Zhejiang Provincial Key Lab of Part Rolling Technology, Ningbo 315211, China*
[3]*Department of Precision Machinery and Precision Instrumentation, University of Science and Technology of China, Hefei 230027, China*
**Corresponding author: majianqiang@nbu.edu.cn*

Received December 12, 2014; accepted January 16, 2015; posted online March 5, 2015

Adaptive optics (AO) systems greatly improve the resolution of retinal imaging instruments by actively correcting ocular aberrations. In this Letter, closed-loop correction as well as ocular aberration compensation of a 62-element silicon unimorph deformable mirror (DM) driven by only positive voltage is performed. The experimental results show that the root-mean square (RMS) wavefront of the initial mirror surface is reduced to 0.011 μm in a closed-loop AO system. The DM reproduces Zernike shapes from the third to 35th mode accurately. The simulated compensation of 200 ocular wavefronts shows that the average RMS value after correction is reduced to 0.017 μm.

OCIS codes: 220.1080, 170.4470, 220.1000.
doi: 10.3788/COL201513.042201.

Retinal imaging in vivo is the fundamental basis for clinical research and patient care in ophthalmology[1]. However, the resolution of retinal imaging is restricted by the aberrations of human eyes. In order to solve this issue, adaptive optics (AO), first developed for astronomy and military applications[2,3], was applied to actively compensate the ocular aberrations in instruments such as an AO scanning laser ophthalmoscope (SLO)[4–6] and AO optical coherence tomography (OCT)[7]. The resolution has been greatly improved. A deformable mirror (DM) as a wavefront corrector determinates the correction capability of the AO system[8–10]. Bimorph/unimorph DMs are suitable for ocular applications, since they are low-cost and have large stroke[11]. Recently, a silicon unimorph DM driven by only positive voltage was developed[12,13], which has potential for ocular applications. In this Letter, we characterize the closed-loop correction capability of this DM with 62 elements. Furthermore, we evaluate the ability of the DM to compensate for the aberrations of the eye using an aberration model reported in Ref. [14].

The silicon unimorph DM consists of a silicon film (300 μm thick) and a lead zirconate titanate (PZT) film (100 μm thick) with the edge supported, as shown in Fig. 1. The DM has an outer ring actuator and a 61 actuator array with a hexagonal arrangement. In order to actuate in both directions, a bias voltage is applied to the ring actuator which produces a concave deformation approximately half of the maximum convex deformation generated by the 61 inner actuators. The 61 inner actuators are utilized to correct aberrations. The optimal active area used for the correcting aberrations is 20 mm in diameter. More details about the design and fabrication of the DM can be found in Ref. [12]. In this work, the bias voltage of the ring actuator is 60 V. The voltage range of the inner actuators is from 0 to 100 V. It should be known that 200 V is also safe for the DM if larger stroke is required for AO applications.

The experimental AO system for closed-loop correction is depicted in Fig. 2. The collimated He–Ne laser beam is expended and passes through the beam splitter (BS), then is reflected by the DM and directed to the beam contractor. After being demagnified, the wavefront of the laser beam is measured by a Shack–Hartman wavefront sensor (WFS, Thorlabs WFS150-5 C). The maximum frame rate of the WFS is 15 Hz. In the work, a lenslet array of 27 × 27 was used. The pattern matching of the DM and WFS is also shown in Fig. 2. The control system [i.e., a personal

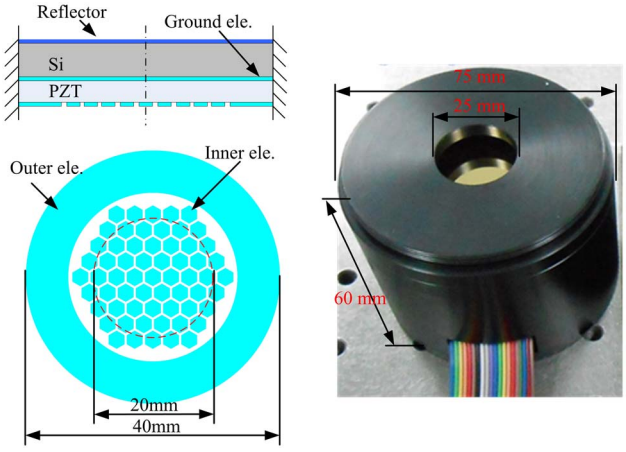

Fig. 1. Silicon unimorph DM. Left, structure of the DM; right, photo of the fabricated DM.

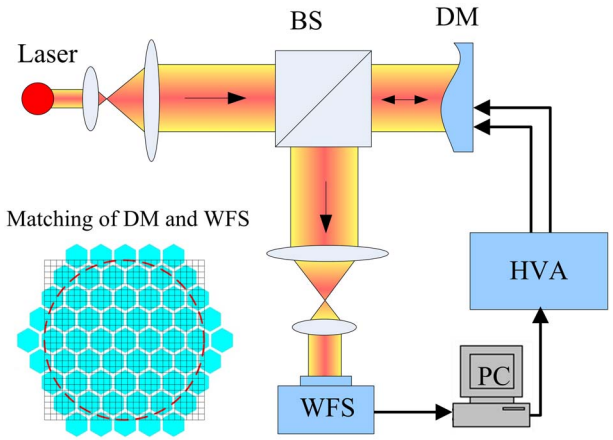

Fig. 2. Experimental setup of the closed-loop correction system.

computer (PC)] uses the wavefront measurements to adjust the surface shape of the DM to reproduce the target wavefront. The high-voltage amplifier (HVA) array has an output range of 0–200 V. The bandwidth of the test system is about 10 Hz.

Figure 3 shows the measured stroke of the central actuator and the ring actuator. As expected, the central actuator generates a local convex deformation with a peak-to-valley (PV) wavefront of 2.3 μm at 50 V. The inter-actuator coupling value is about 48%. The ring actuator generates a whole concave defocus deformation. The PV wavefront is 16.6 μm at 60 V, and the corresponding root-mean square (RMS) value is 4.76 μm. The first-order resonance frequency of the DM is about 2.4 kHz measured using a laser Doppler vibrometer (LDV).

The mirror deformation can be controlled by the voltage of the actuators and the linear relationship is given by

$$A = \mathbf{BV}, \tag{1}$$

where A is the mirror deformation (wavefront) expressed as Zernike polynomial coefficients, $\mathbf{V}$ is a vector of the voltages applied to the actuators, and $\mathbf{B}$ is the influence function matrix that contains all the spatial information of the DM. The influence function matrix is measured by sequentially applying voltages to each actuator and measuring the corresponding response of the mirror deformation. In order to evaluate the capability of the DM, a closed-loop control algorithm proposed in Ref. [15] was used.

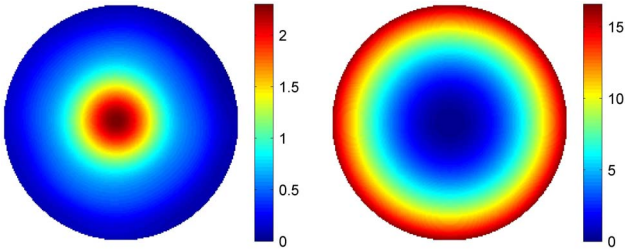

Fig. 3. Stroke of the DM. Left, central actuator at 50 V; right, ring actuator at 60 V.

The iterative formula based on steepest descent algorithm is expressed as

$$\mathbf{V}_{(n)} = \mathbf{V}_{(n-1)} - 2\mu\mathbf{B}^{\mathrm{T}}(A_{(n-1)} - A_{\mathrm{target}}), \tag{2}$$

where n is the iteration number, A_{target} is the target wavefront to be generated, and μ is a positive coefficient that affects the convergence speed. The residual wavefront error between the mirror surface and target wavefront reduces monotonically with iteration number.

The correction of the initial mirror surface in closed-loop form is shown in Fig. 4. The PV wavefront of the initial mirror surface is 5.8 μm, and the RMS value is 0.86 μm. The RMS residual wavefront decreases quickly with the iterations. More than 95% of the total aberrations can be corrected within two to three iterations. After 40 iterations the residual wavefront error is stable and corresponds to the best solution. The PV wavefront is reduced to 0.119 μm and the RMS wavefront is 0.011 μm ($\sim\lambda/60$, $\lambda = 600$ nm).

Additionally, the Zernike shapes from to the third to 35th mode were reproduced in the voltage range of 0–100 V. Figure 5 shows that the experimentally reproduced shapes are in accordance with the theoretical shapes excellently. The corresponding RMS wavefront and RMS residual wavefront error of each reproduced Zernike shape are calculated and are shown in Fig. 6. As expected for a unimorph DM, the low-order Zernike shapes reproduced have large amplitude, especially for the defocus mode of which the RMS wavefront is approximately 2.8 μm. Most of the residual wavefront errors are less than 0.03 μm RMS. The normalized residual errors are less than 0.05 for the first nine mode shapes. The closed-loop correction of the mirror surface and the reproduction of the Zernike shapes demonstrate that this silicon unimorph DM has potentially excellent performance for ocular and other applications[9].

A simulation of the compensation of ocular aberrations was also performed. A statistical model proposed in

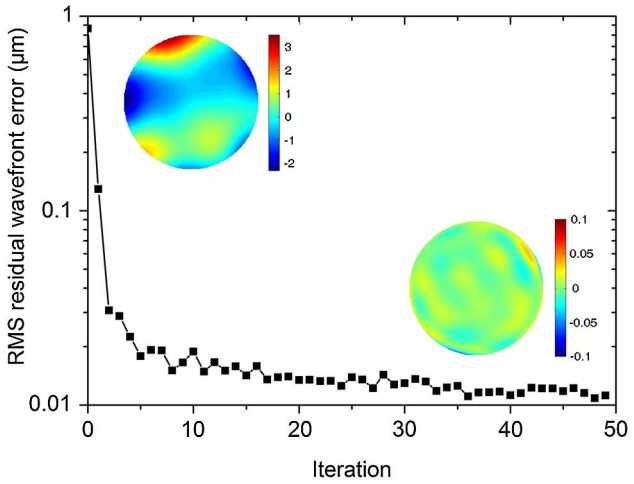

Fig. 4. Closed-loop correction of the initial mirror wavefront. Insets, mirror wavefront before and after correction.

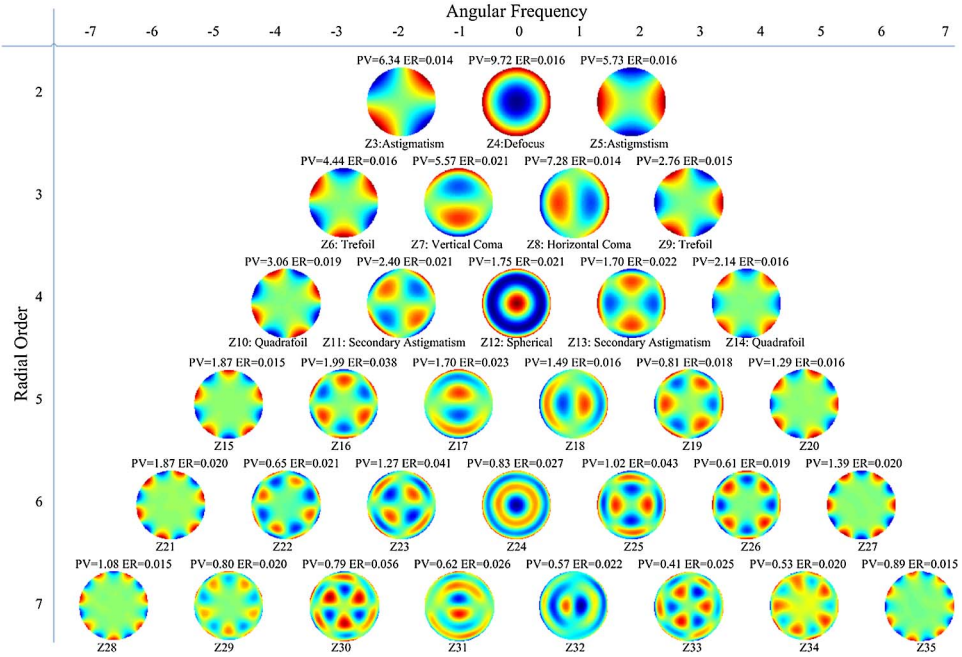

Fig. 5. Zernike shapes from the third to 35th mode reproduced in closed-loop form. PV refers to PV wavefront and ER refers to RMS wavefront residual error.

Ref. [14] was used to simulate the aberrations of human eyes. In this model, ocular aberration is described by a multivariate Gaussian random vector of Zernike coefficients with known mean, variance, and covariance. In this work, the pupil of the eye was set as 6 mm. First we simulated 200 ocular wavefronts using the first 36 modes of the Zernike polynomials (piston and tip/tilt modes were removed). Then these ocular wavefronts were compensated using the measured influence function matrix. The correction results show that all these eyes are corrected significantly, as shown in Fig. 7. The average RMS value of the ocular wavefronts is 0.671 μm with a standard deviation (SD) of 0.258 μm, which is reduced to 0.017 μm with 0.006 μm SD after correction by the DM. The Strehl ratio (SR) defined as the ratio of peak diffraction intensities of an aberrated versus perfect wavefront was also calculated as per[16]

$$\mathrm{SR} = \mathrm{e}^{-\left(\frac{2\pi\sigma}{\lambda}\right)^2}, \tag{3}$$

where σ is the RMS residual ocular wavefront error. $\mathrm{SR} > 0.8$ is usually taken to mean that the system achieves diffraction-limited performance. After correction, the mean of SR is 0.965 with a SD of 0.024, which indicates that the DM has diffraction-limited performance.

Several comparisons of commercial DMs have been reported for ocular AO applications[16,17]. In Ref. [16], eight commercial DMs were compared by simulation. The 52 element magnetic DM from Imagine Eyes (MIRAO52) has the best performance with an average RMS residual

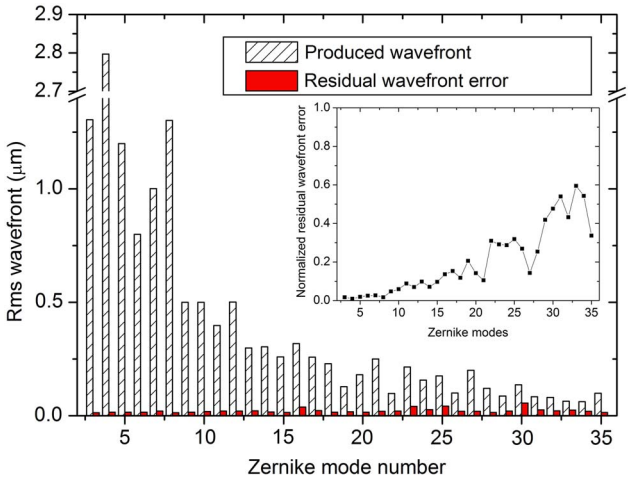

Fig. 6. RMS wavefront and RMS residual wavefront error of the reproduced Zernike shapes. Inset, normalized residual wavefront error.

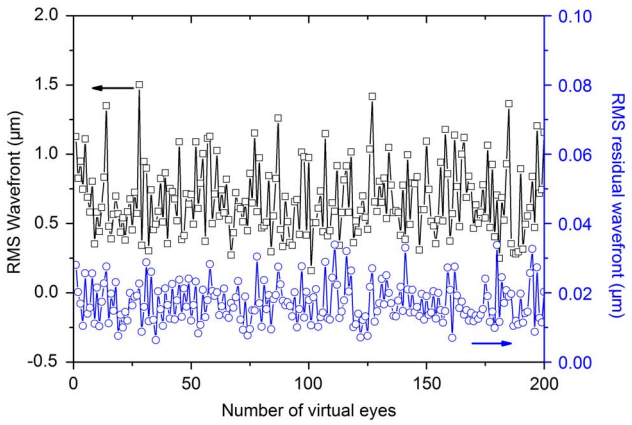

Fig. 7. RMS ocular wavefront aberrations before and after correction (without piston and tip/tilt).

wavefront of ∼0.02 μm. The aperture of MIRAO52 is 15 mm. The individual and whole strokes (wavefront) are >20 and 50 μm, respectively. Although the stroke of the proposed DM in this Letter is smaller than that of MIRAO52, the simulation results show that the DM has a comparable performance for 6 mm ocular AO applications, since the DM has sufficient stroke and more actuators. Additionally, the aperture of 20 mm does not match the pupil of the eye which is less than 10 mm[9].

In conclusion, the closed-loop correction performance and the compensation of ocular aberrations using a silicon unimorph DM with 62 elements are evaluated. A closed-loop AO system with a WFS is built. The RMS wavefront of initial mirror surface is reduced from 0.86 to 0.011 μm after the closed-loop correction. The DM reproduces Zernike shapes from the third to 35th mode accurately with a normalized residual wavefront less than 0.05 for the first nine modes. Compensation simulation of 200 ocular wavefronts shows that the ocular wavefront can be reduced to a 0.017 μm RMS value, and the corresponding SR is 0.965. The results demonstrate that the proposed silicon unimorph DM is suitable for ocular AO applications.

This work was supported by the National Natural Science Foundation of China (11303019), the Zhejiang Provincial Natural Science Foundation of China (LQ13E050016), the Ningbo Natural Science Foundation (2013A610047), and the Project of Education Department of Zhejiang Province (Y201326728). The authors also thank the support of the K. C. Wong Magna Fund in Ningbo University.

References

1. Y. He, H. Li, J. Lu, G. Shi, and Y. Zhang, Chin. Opt. Lett. **11**, 021101 (2013).
2. P.-Y. Madec, Proc. SPIE **8447**, 844705 (2012).
3. J. Mu, W. Zheng, M. Li, and C. Rao, Chin. Opt. Lett. **10**, 120101 (2012).
4. A. Roorda, J. Vision **11**, 6 (2011).
5. J. W. Zhou, Y. D. Zhang, Y. Dai, H. X. Zhao, R. Liu, F. Hou, B. Liang, R. F. Hess, and Y. F. Zhou, Nat. Sci. Rep. **2**, 364 (2012).
6. Y. Yu and Y. Zhang, Chin. Opt. Lett. **12**, 121202 (2014).
7. Y. Jian, J. Xu, M. A. Gradowski, S. Bonora, R. J. Zawadzki, and M. V. Sarunic, Biomed. Opt. Express **5**, 547 (2014).
8. Q. Q. Mu, Z. L. Cao, D. Y. Li, L. F. Hu, and L. Xuan, Opt. Express **15**, 1946 (2007).
9. N. Doble and D. R. Williams, IEEE J. Sel. Top. Quantum Electron. **10**, 629 (2004).
10. S. S. Niu, J. X. Shen, C. Liang, Y. H. Zhang, and B. M. Li, Spectrosc. Spect. Anal. **32**, 1795 (2012), in Chinese.
11. D. A. Horsley, H. Park, S. P. Laut, and J. S. Werner, Sens. Actuator A Phys. **134**, 221 (2007).
12. J. Q. Ma, Y. Liu, T. He, B. Q. Li, and J. R. Chu, Appl. Opt. **50**, 5647 (2011).
13. J. Q. Ma, K. Chen, J. J. Chen, and J. R. Chu, Proc. SPIE **9298**, 92981E (2014).
14. L. N. Thibos, Ophthal. Phys. Opt. **29**, 288 (2009).
15. L. J. Zhu, P. C. Sun, D. U. Bartsch, W. R. Freeman, and Y. Fainman, Appl. Opt. **38**, 168 (1999).
16. N. Devaney, E. Dalimier, T. Farrell, D. Coburn, R. Mackey, D. Mackey, F. Laurent, E. Daly, and C. Dainty, Appl. Opt. **47**, 6550 (2008).
17. E. Dalimier and C. Dainty, Opt. Express **13**, 4275 (2005).